Applied Mechanics and Materials Vol. 82 (2011) pp 344-349
Online available since 2011/Jul/27 at www.scientific.net

doi:10.4028/www.scientific.net/AMM.82.344

Effects of Outrigger Truss Systems on Collapse Initiation Times of High-Rise Towers Exposed to Fire

Daigoro Isobe[1,a] and Le Thi Thai Thanh[2,b]

[1]Associate Professor, Univ. of Tsukuba, 1-1-1 Tennodai, Tsukuba-shi, Ibaraki 305-8573, Japan

[2]Graduate student, Univ. of Tsukuba, 1-1-1 Tennodai, Tsukuba-shi, Ibaraki 305-8573, Japan

[a]isobe@kz.tsukuba.ac.jp, [b]e0712356@edu.esys.tsukuba.ac.jp

Keywords: Outrigger truss system, Collapse initiation time, High-rise towers, Fire, Progressive collapse, ASI-Gauss technique.

Abstract. In this paper, progressive collapse analyses were performed on a 30-story, seven-span tower that was exposed to fire. The Adaptively Shifted Integration (ASI)-Gauss technique was used to demonstrate the effects of fire patterns and structural parameters on collapse initiation time: the duration from the beginning of the fire until collapse initiation. Specifically, an outrigger truss system was placed on the roof of a model, and the influence of the system on the structural vulnerability of the tower was verified. The structural parameters that were varied in the analyses included the axial force ratio, the member joint strength ratio and the member strength ratio of the outrigger trusses to the strength of the beams on the first floor. From the numerical results, it is confirmed that collapse initiation times are significantly affected by the member joint strength ratio if the axial force ratio is small (floor loads are low) on the condition that the fire pattern is nearly symmetrical, and the load paths to and from the outrigger truss system are sufficiently protected.

Introduction

Studies on the resistance of buildings to collapse are becoming increasingly prominent because the number of decrepit buildings has increased worldwide. The desire of researchers to assess the performance of buildings under stress has been increasing since the 9.11 terrorist attacks on the World Trade Center (WTC) towers in 2001. To determine the true cause of the total collapse of these towers, we conducted an aircraft impact analysis [1] followed by fire-induced collapse analyses to investigate how fire patterns, the structural weakness of member joints, and the outrigger trusses on roof tops influenced the collapse behavior of the high-rise towers [2]. The analytical results of the latter analyses, which were obtained using the Adaptively Shifted Integration (ASI)-Gauss finite element code [3], showed a clear difference between each fire pattern, between the models with strong and weak member-joint strengths, and between the models with and without outrigger trusses. In general, the strongly designed models withstood total collapse, whereas the weak models began to collapse when the temperature was highest, which eventually resulted in total collapse. The models with outrigger trusses tended to withstand collapse longer due to their catenary action only if their load paths were protected. In this paper, we focused on the change of collapse initiation time: the duration from the beginning of the fire until the beginning of the collapse, when structural parameters such as the axial force ratio, the member joint strength ratio and the member strength ratio of the outrigger trusses to the strength of beams on the first floor were varied. An outline of the numerical code is first described, followed by numerical results and discussion.

Numerical Methods

Relationship between the location of the numerical integration point in a linear Timoshenko beam element and the stress evaluation point where a plastic hinge is formed in a rigid bodies-spring model (RBSM) is expressed as

$$r = -s, \tag{1}$$

where *s* is the location of the numerical integration point and *r* is the location where the stress and strain are evaluated or the location of a plastic hinge in the plastic stage. The *s* and *r* terms are dimensionless quantities with values between -1 and 1.

In both the ASI and ASI-Gauss techniques, the numerical integration point is shifted adaptively if a fully plastic section is formed within an element. When the plastic hinge is unloaded, the corresponding numerical integration point shifts back to its original position. Here, the original position represents the location where the numerical integration point is placed if the element behaves elastically. Therefore, the plastic behavior of the element is simulated appropriately, and a converged solution is achieved using only a small number of elements per member. However, in the ASI technique, the numerical integration point is placed at the midpoint of the linear Timoshenko beam element, which is considered to be optimal for one-point integration if the entire region of the element behaves elastically. Therefore, solutions in the elastic range are not sufficiently accurate if the number of elements per member is very small because a low-order displacement function is applied for the linear Timoshenko beam element.

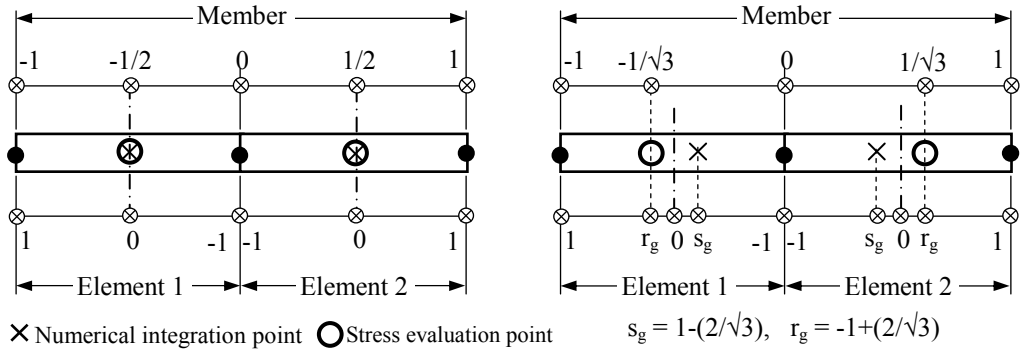

(a) ASI technique (b) ASI-Gauss technique

Fig. 1 Location of numerical integration and stress evaluation points in the elastic range

The primary difference between the ASI and ASI-Gauss techniques is the original position of the numerical integration point as shown in Fig. 1. In the ASI-Gauss technique, two consecutive elements that form a member are considered to be a subset, and the numerical integration points of an elastically deformed member are located such that the stress evaluation points coincide with the Gaussian integration points ($\pm 1/\sqrt{3}$ in dimensionless coordinate) of the member. Thus, the stress and strain are evaluated at the Gaussian integration points of the elastically deformed members. The Gaussian integration points are optimal for two-point integration, and the accuracy of the bending deformation is mathematically guaranteed [4]; therefore, the ASI-Gauss technique takes advantage of two-point integration while utilizing one-point integration in the actual calculations.

Figure 2 shows the location of the numerical integration points for each stage of the ASI-Gauss technique. A plastic hinge is typically generated before it develops into a member fracture, and the plastic hinge is expressed by shifting the numerical integration point to the opposite end of the fully plastic section according to Eq. 1. For instance, if a fully plastic section initially occurs at the right end of an element ($r = 1$) as shown in Fig. 2, then the numerical integration point shifts immediately to the left end of the element ($s = -1$). At the same time, the numerical integration point of the adjacent element that forms the same member is shifted back to its midpoint where it is appropriate for one-point integration. A member fracture is expressed by reducing the sectional forces of the element immediately after the occurrence of a fractured section on either end of the element.

The yield condition used in the analyses is expressed as follows:

$$f = \left(\frac{M_x}{C_M M_{x0}}\right)^2 + \left(\frac{M_y}{C_M M_{y0}}\right)^2 + \left(\frac{N}{N_0}\right)^2 - 1 = f_y - 1 = 0, \tag{2}$$

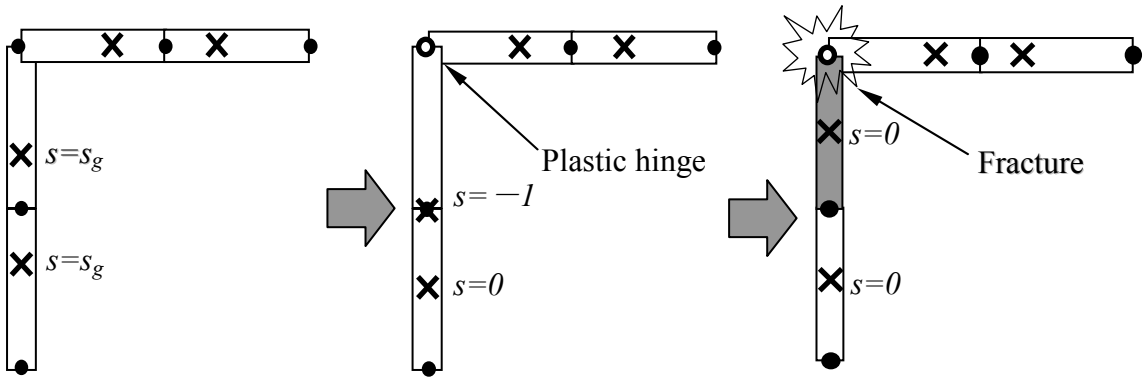

(a) Elastic stage (b) Plastic stage (c) Member fracture

Fig. 2 Location of numerical integration points for each stage of the ASI-Gauss technique

where f_y is the yield function, M_x, M_y and N are the bending moments around the x and y axis and the axial force, respectively. The terms with the subscript 0 are values that result in a fully plastic section in an element if they act on the cross section independently. The parameter C_M, which represents the ratio of the member joint strength to the strength of the member itself, is used to explicitly express the influence of the member joint strength. The values of the ratio are fixed on the basis that the member joint strengths of some of the columns in the WTC towers were weak compared to those of the members [5].

The fracture condition of the member joints is considered by examining the bending strains, axial tensile strain and shear strains in a member as follows:

$$\left|\frac{\kappa_x}{\kappa_{x0}}\right| - 1 \geq 0 \quad or \quad \left|\frac{\kappa_y}{\kappa_{y0}}\right| - 1 \geq 0 \quad or \quad \left|\frac{\gamma_{xz}}{\gamma_{xz0}}\right| - 1 \geq 0 \quad or \quad \left|\frac{\gamma_{yz}}{\gamma_{yz0}}\right| - 1 \geq 0 \quad or \quad \left(\frac{\varepsilon_z}{\varepsilon_{z0}}\right) - 1 \geq 0, \tag{3}$$

where κ_x, κ_y, γ_{xz}, γ_{yz}, ε_z, κ_{x0}, κ_{y0}, γ_{xz0}, γ_{yz0} and ε_{z0} are the bending strains around the x and y axis, the shear strains for the x and y axis, the axial tensile strain and the critical values for these strains, respectively. We used critical fracture strains, which were obtained from experiments on high-strength joint bolts [6].

Elemental contact is considered in the numerical code by connecting gap elements between the pairs of elements that are determined to be in contact by their geometrical relationships. More details regarding the code can be found in [3] and [7].

Fire-Induced Progressive Collapse Analyses for the High-Rise Towers

Fire-induced collapse analyses were performed on a 30-story, seven-span tower as shown in Fig. 3. An outrigger truss system was placed on the roof of the model, and the influence of the system on the structural vulnerability of the tower was verified. Several structural parameters were varied to determine their contribution to the collapse behavior: the axial force ratio of the columns to the structural strength capacity varied from 0.1 to 0.5, which was determined by varying only the floor loads; the member joint strength ratio C_M at every member connection in the model varied from 0.1 to 0.6; and the member strength ratio of the outrigger trusses to the strength of beams on the 1st floor varied from 0.0 (no outrigger truss system placed) to 2.0. The tower model consisted of 9,360 linear Timoshenko beam elements, 6,644 nodes and 39,600 degrees of freedom. For example, the columns used on the 1st floor were 700 mm × 700 mm box-section-type steel columns with 28-mm-thick plates. Two fire patterns were applied: three rows of sections in the middle and the sections in the outer area, from the 21st to the 24th floors were assumed to be on fire, as shown in Fig. 4, to determine how the fire patterns affected the collapse initiation time. The aircraft collision followed by

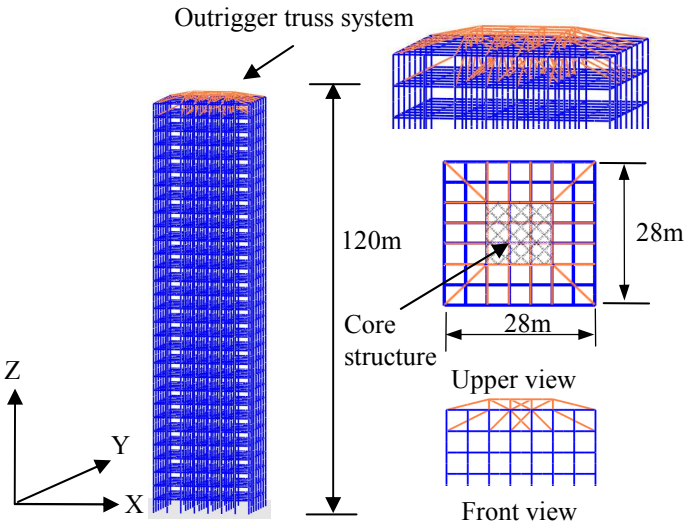

Fig. 3 30-story, seven-span tower model

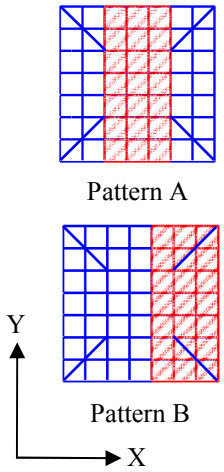

Fig. 4 Assumed fire patterns (21F-24F)

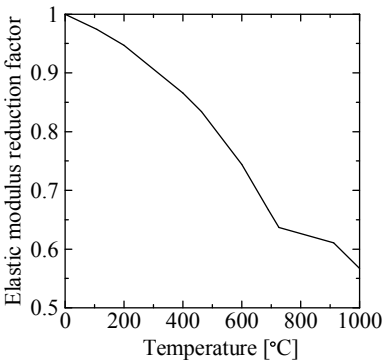

(a) Elastic modulus

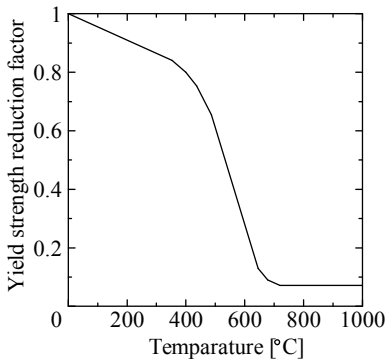

(b) Yield strength

Fig. 5 Strength reduction curves of raw steel due to elevated temperatures [8]

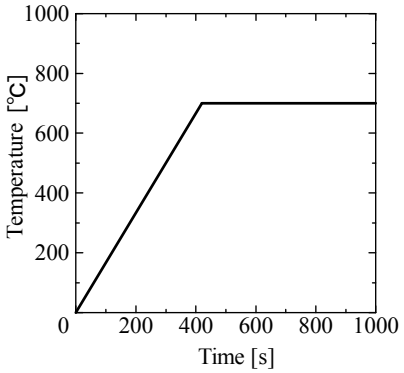

Fig. 6 Assumed time history of temperature

explosions due to jet fuel was assumed to dislodge the thermal insulation in the WTC incident. Therefore, reduction curves [8] were adopted for the elastic modulus and the yield strength of raw steel due to the elevated temperatures as shown in Fig. 5. It was found that the elastic modulus of the columns with no thermal insulation reduced to 60 % of its original value, and the yield strength reduced to 10 % of its original strength at 700 degrees Celsius, which is a typical temperature in a fire. The temperature of the beam elements in the ranges indicated in Fig. 4 was assumed to have increased to 700 degrees Celsius in seven minutes as shown in Fig. 6. In addition, a time increment control was applied to enable continuous calculation from static to dynamic phenomena. The analysis required approximately eight hours of simulation time using a personal computer (CPU: 2.93 GHz Xeon).

Figures 7 and 8 show the collapse modes of the tower exposed to each fire pattern when the member joint strength ratio C_M was set to 0.3 and the axial force ratio in the columns of the 1st floor was set to 0.33 with the regular-strength outrigger truss system (structural strength similar to the beams on the 1st floor) placed on the roof. The colors of the elements indicate the f_y values in Eq. 2. In all of the cases, total collapse was inevitable, and the results clearly show the effect of the weakness of the member joints compared to the fully rigid joints and the effect of the strength reduction due to the elevated temperatures. As shown in the figures, the collision of the upper structure with the lower structure created shock waves that propagated through the columns and moved faster than the falling motion of the upper structure. The shock waves destroyed the member joints as they moved towards

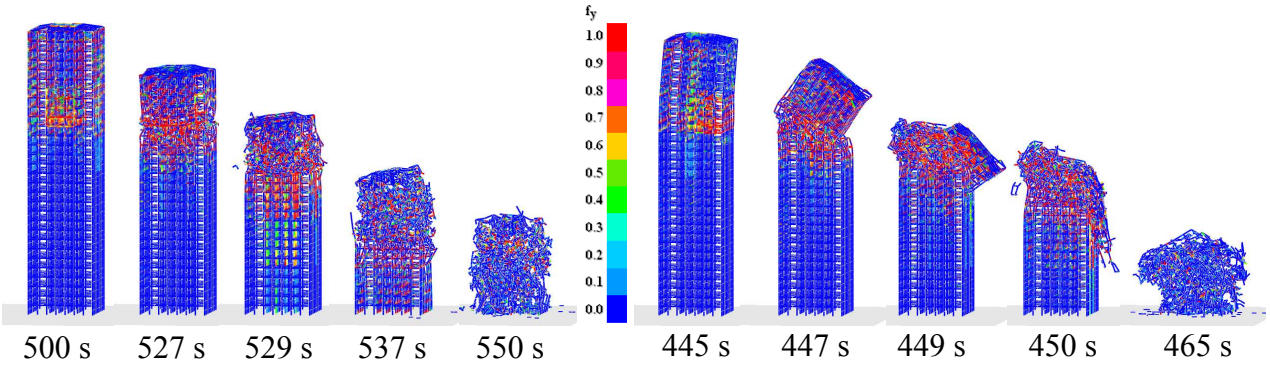

Fig. 7 Collapse mode (C_M= 0.3, axial force ratio = 0.33, fire pattern A)

Fig. 8 Collapse mode (C_M= 0.3, axial force ratio = 0.33, fire pattern B)

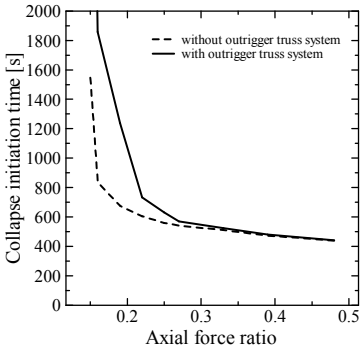

(a) Fire pattern A

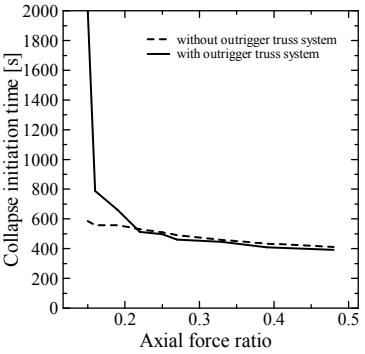

(b) Fire pattern B

Fig. 9 Collapse initiation time vs. the axial force ratio

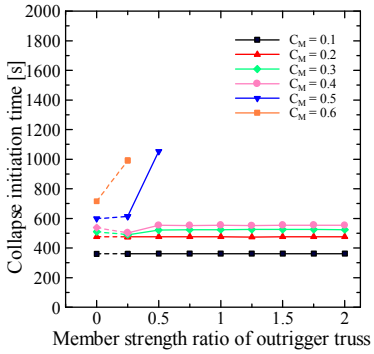

(a) Fire pattern A

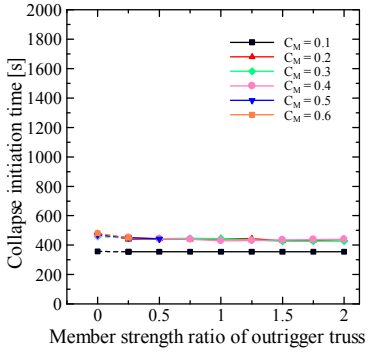

(b) Fire pattern B

Fig. 10 Influence of structural parameters on the collapse initiation time (axial force ratio= 0.33)

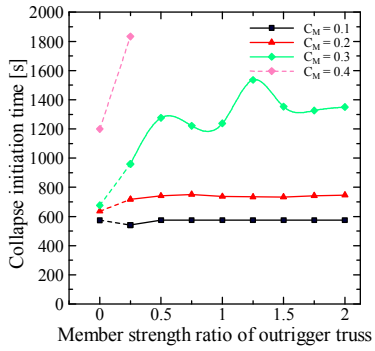

(a) Fire pattern A

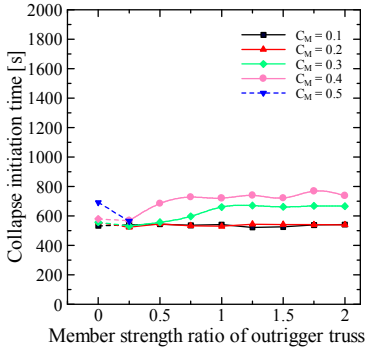

(b) Fire pattern B

Fig. 11 Influence of structural parameters on the collapse initiation time (axial force ratio= 0.19)

the ground level. The fire patterns did not appear to affect the overall collapse behavior; however, the slant angles at the collapse initiation phase were different, and the collapse initiation time was shorter if the fire pattern was asymmetrical. The collapse initiation time depends on the strength and the number of outrigger trusses that support the load paths near the structural deficiencies. Figure 9 shows the relationship between the collapse initiation time and the axial force ratio. The collapse initiation time was not affected by the presence of the outrigger truss system if the axial force ratio was larger. However, the effect of the outrigger truss system on the collapse initiation time increased in all of the cases if the axial force ratio had small values. Therefore, the influence of the structural parameters on the collapse initiation time were investigated and compared in two different cases: (1) axial force ratio=0.33 (floor load: 10.0 kN/m^2) where the difference of collapse initiation times was smaller and (2) axial force ratio=0.19 (floor load: 5.0 kN/m^2) where the difference was larger. Figure 10 shows the results for the former case. The results without plots are the cases in which the tower model did not

collapse throughout the entire calculation time. Although the greater strength of the outrigger trusses and the member joints slightly increased the collapse initiation time for fire pattern A, it did not appear to significantly affect the collapse initiation time if the fire pattern became asymmetrical as in fire pattern B. In particular, each of the cases, except for the case where C_M =0.1, exhibited a constant collapse initiation time of around 450 s when fire pattern B was applied (Fig. 10(b)). Figure 11 shows the results for the latter case when the floor loads were smaller. The collapse initiation time appears to be largely affected by the presence of the outrigger truss system. However, the member strength of the outrigger truss is not the most significant parameter. In this case, the member joint strength ratio C_M is the most significant parameter. For example, the collapse initiation time with C_M =0.2 under fire pattern A varies approximately 80 s between the models with and without the outrigger truss system, while the collapse initiation time with C_M =0.3 increases for about 600 s if the system is present.

These results confirmed that the collapse initiation times can be significantly affected by the member joint strength ratio, particularly if the axial force ratio is small (floor loads are low), under the condition that the fire pattern is nearly symmetrical and the load paths to and from the outrigger truss system are sufficiently protected.

Conclusion

The numerical results of this paper indicate that the collapse initiation time of a high-rise tower with an outrigger truss system depends on fire patterns. The outrigger truss system delays the time until collapse initiation in the models with a smaller axial force ratio, a member joint strength ratio of 0.3 or greater and for symmetrical fire patterns.

We plan to perform further investigations using full-scale, fire-induced collapse analyses of the WTC towers.

References

[1] D. Isobe and Z. Sasaki: Aircraft Impact Analyses of the World Trade Center Towers, *CD-ROM Proceedings of the 1st International Workshop on Performance, Protection, and Strengthening of Structures under Extreme Loading (PROTECT2007)*, (2007), Whistler, Canada.

[2] D. Isobe, H. Yokota and L. T. T. Thanh: Fire-Induced Progressive Collapse Analyses of High-Rise Towers, *CD-ROM Proceedings of the 2nd International Workshop on Performance, Protection, and Strengthening of Structures under Extreme Loading (PROTECT2009)*, (2009), Hayama, Japan.

[3] K.M. Lynn and D. Isobe: in *Int. J. for Numerical Methods in Engineering*, Vol. 69, No. 12, (2007), pp.2538-2563.

[4] W.H. Press, S.A. Teukolsky, W.T. Vetterling and B.P. Flannery: *Numerical recipes in FORTRAN: The art of scientific computing*, New York: Cambridge University Press, (1992).

[5] ASCE/FEMA, *World Trade Center Building Performance Study: Data Collection, Preliminary Observation and Recommendations*, (2002).

[6] T. Hirashima, N. Hamada, F. Ozaki, T. Ave and H. Uesugi: in *J. Struct. Constr. Eng., AIJ*, Vol. 621**,** (2007), pp. 175-180, in Japanese.

[7] Y. Toi and D. Isobe: in *Int. J. for Num. Methods in Engineering*, Vol. 36, (1993), pp.2323-2339.

[8] NIST NCSTAR 1: *Federal Building and Fire Safety Investigation of the World Trade Center Disaster: Final Report on the Collapse of the World Trade Center Towers*, National Institute of Standards and Technology (NIST), (2005).

Performance, Protection and Strengthening of Structures under Extreme Loading
doi:10.4028/www.scientific.net/AMM.82

Effects of Outrigger Truss Systems on Collapse Initiation Times of High-Rise Towers Exposed to Fire
doi:10.4028/www.scientific.net/AMM.82.344